JOURNAL OF MATERIALS SCIENCE **33** (1998) 5291–5300

Relationship between strength and failure mode of ceramic multilayers

BENT F. SØRENSEN, SØREN PRIMDAHL
Materials Research Department, Risø National Laboratory, DK-4000 Roskilde, Denmark

The mechanical strength of ceramic multilayers for use in solid oxide fuel cell stacks was examined. The multilayers consist of a substrate, made of yttria stabilised zirconia (YSZ), with a NiO/YSZ composite coating on both faces. Under some processing conditions the mechanical strength of the multilayers was similar to that of pure YSZ, while a much lower strength was found for other processing conditions. Inspections of the fracture surfaces revealed markedly different appearances, suggesting that a transition in failure mode had occurred. Fracture mechanics models for thin films on substrates were used to interpret the observed fracture modes, providing insight to the underlying failure mechanisms.

1. Introduction

This paper concerns the relationship between the processing conditions and failure mode of ceramic multilayers. Often, ceramic multilayers are designed primarily from a functional point of view. However, such components must have a certain mechanical strength, such that they do not fracture during handling or use. A certain understanding of the fracture mechanisms is thus required. As an example, solid oxide fuel cell (SOFC) stacks may consist of various layers of sintered ceramic materials, each chosen to serve specific functional purposes [1]. Incidentally, most of these materials have low fracture energy. Ceramic multilayers are usually sintered together at a high temperature. Since the materials have different thermal expansion coefficients, residual stresses may exist in the layers at room temperature, as each layer cannot contract freely during cool down after sintering. The residual stresses may cause cracking of layers or delamination. From a functional point of view it is attractive to have a good contact and strong bonding between the layers, such that the contact resistance is minimised. Intuitively, perhaps, one would think that a strong bonding between the layers would give a high mechanical strength. But is that always right? This question will be addressed in this paper.

There are few studies focusing on the fracture mechanical behaviour of materials for SOFCs. Of these, nearly all studies concern characterisation of the individual materials, such as the measurement of the fracture energy of materials for electrolytes and interconnetors [2–6]. However, as will be shown in the following, a critical issue is the interfacial bonding between the layers.

The present study focuses on a problem encountered for an yttria-stabilised zirconia (YSZ) electrolyte coated with a NiO/YSZ composite. In short, the problem is that under certain process conditions this multilayer exhibits a much lower mechanical strength than the blank YSZ electrolyte, while under other process conditions the strength of the coated YSZ is retained. The present work is intended to uncover the reason for this loss of strength by (i) a characterisation of fracture mode from observations of fracture surfaces and (ii) by the use of existing fracture mechanics models for cracking of coatings on substrates.

2. Experimental procedure

2.1. Processing of multilayers

Electrolyte substrates were made from YSZ (Tosoh, ZrO_2 with 8 mol % Y_2O_3) processed by tape casting. Green foils were cut to measure 50×50 mm^2 and sintered at 1350 °C for 8 hours to reach a relative density in excess of 98% and a thickness in the range of 150 to 165 μm. The substrates appeared smooth and without visually detectable flaws.

A 50 to 60 μm thick NiO/YSZ composite layer was applied to both sides of the substrates by spray painting. The slurry, containing NiO and YSZ in the volume ratio 53/47, was prepared as follows. Green NiO and YSZ (Tosoh, ZrO_2 with 8 mol % Y_2O_3) powders were suspended in ethanol by a dispersant (polyvinyl pyrrilidone) [7]. After deagglomeration in a ball mill, the YSZ particle size was about 0.4 μm. After addition of the NiO and further ball milling, the combined particle size distribution was bimodal with fractions of approximately 0.4 μm and 10 μm in the volume ratio 6 : 1. The slurry was sprayed onto both sides of the substrate in three layers of 10 to 20 μm. After deposition of each layer the specimens were sintered for 2 hours. The sintering temperature was 1100 °C for one specimen and 1300 °C for two other specimens. One of the latter specimens was subsequently heated to 1500 °C for two hours.

2.2. Microstructural characterisation

The specimens were examined in an environmental scanning electron microscope (ESEM). The specimens were broken (bending by hand) just before they were inserted into the vacuum chamber. The (uncoated) specimens were mounted such that the side of the fracture surfaces that had been subjected to tensile stress appears to the right side in the micrographs.

3. Experimental results

3.1. Observations of coating and fracture surfaces

The specimens sintered at 1100 °C felt rather strong; similar to blank YSZ specimens. Fig. 1 shows (a) the appearance of the coating and (b) the fracture surface. Large pores (sometimes referred to as 'mud-cracks') are seen in the coating. The shape of the pore edge at one side is different from that at the other side. The opening of these pores is of the order of hundreds of microns. These features indicate that the 'mud-cracks' have formed during drying of the slurry or during sintering. They are therefore classified as pores rather than cracks (cracks have truly sharp crack tips). The substrate has a fairly planar fracture surface (Fig. 1b). This is similar to the fracture surfaces of blank YSZ. The coatings (Fig. 1b) have broken in a much more zigzag manner, perhaps originating from the pores. Delamination between the coating and the substrate has occurred.

Parts of a specimen sintered at 1300 °C are shown in Fig. 2. For these specimens the strength felt much lower. Beside the 'mud-crack' type of pores, cracks are seen in the coating (Fig. 2a). The path of two associated crack faces follows each other exactly, indicating

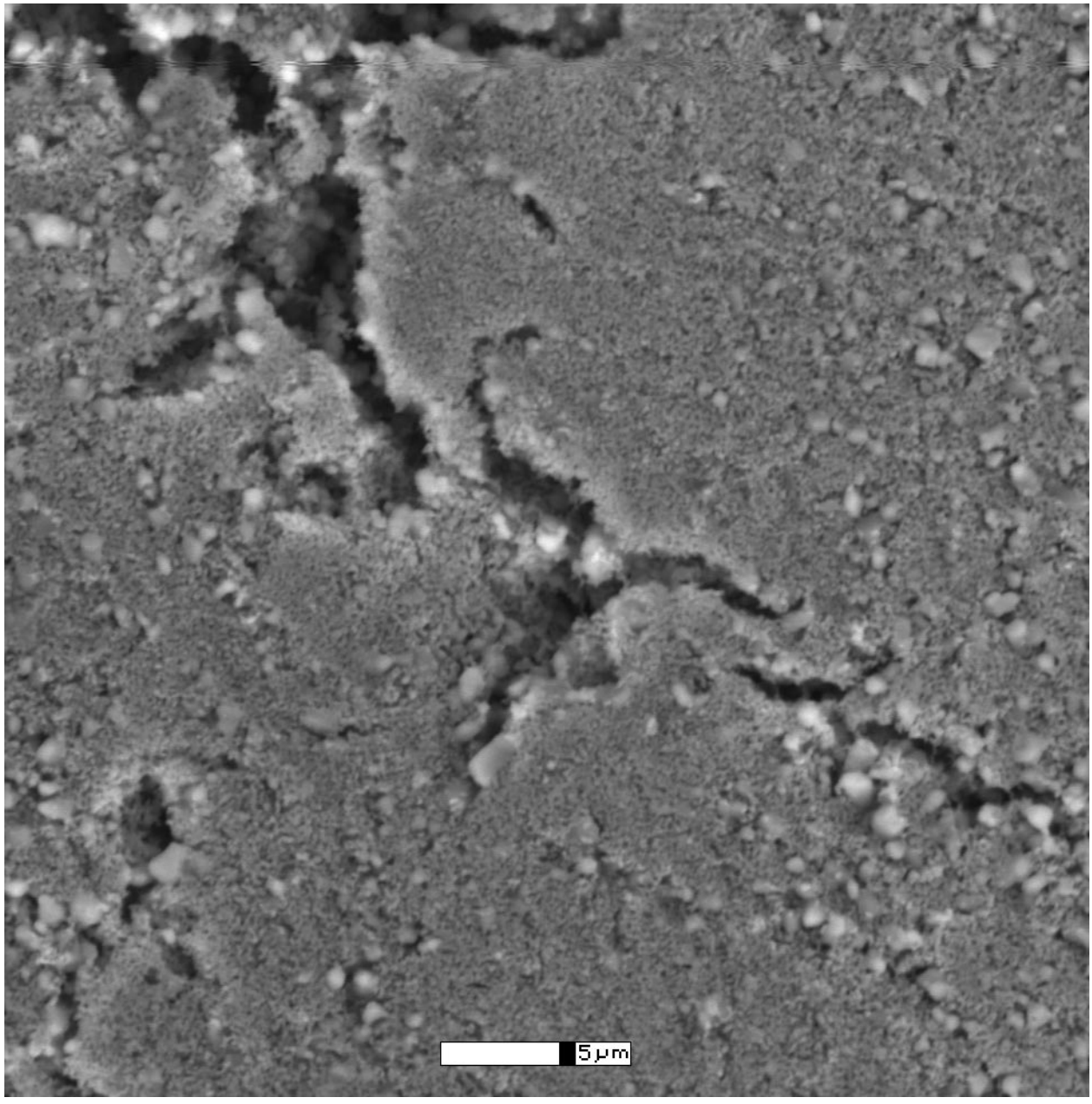

(a)

Figure 1 ESEM micrographs of a specimen sintered at 1100 °C, showing (a) the surface of the coating, and (b) the fracture surface. The fracture surface of the substrate is planar, unlike the fracture surface of the coatings. Note also the evidence of interfacial debonding (delamination).

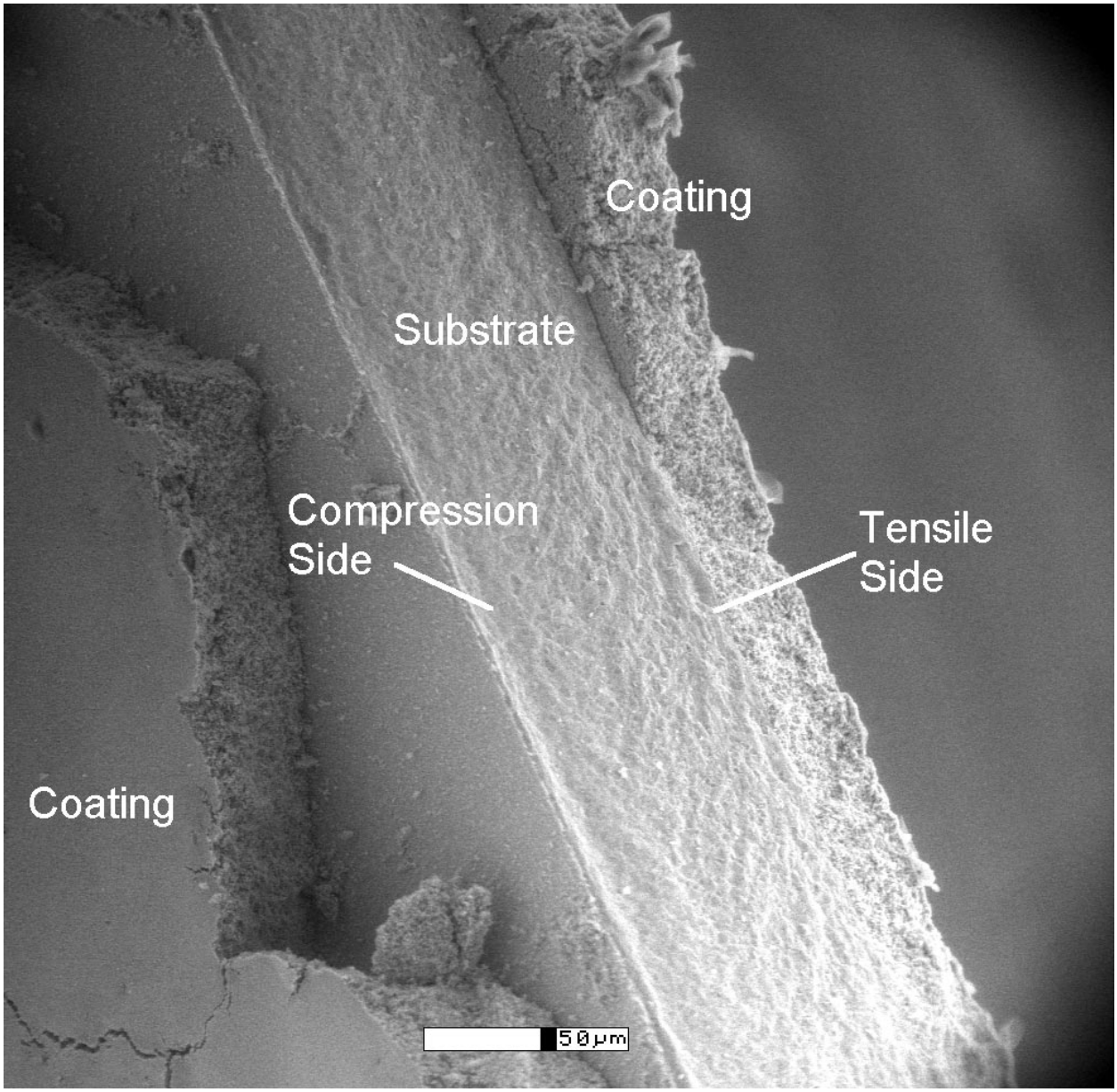

(b)

Figure 1 (Continued)

that no inelastic deformation has taken place since the crack faces separated. Thus, these cracks must have developed after sintering. This type of cracks is denoted 'channel cracks', since they extend over large in-plane distances, but extend only to a small depth [8]. The fracture surface (Fig. 2b) is distinctively different from that of specimens sintered at 1100 °C. In this case the fracture surface of the substrate (the YSZ layer) is much more irregular. In fact, the fracture surface of the substrate follows the fracture surface of the coating layers. No delamination has occurred between the substrate and coating. Note that there is a narrow zone at the boundaries of the substrate (against the coating) which has a different appearance than the central region of the substrate. As will be elaborated later, this region of the fracture surface is likely to have formed during cool down, i.e., channel cracks that have propagated from the coating into the substrate.

The specimen sintered at 1500 °C felt even weaker than those sintered at 1300 °C. The coating, Fig. 3a, contains a lot of channel cracks. The fracture surface, Fig. 3b, was roughly similar to that observed at specimens sintered at 1300 °C. Here the boundary zone has extended a bit further down into the substrate. At some locations cracks were observed to propagate into the substrate and bend 90°, growing parallel with the interface (Fig. 4).

3.2. Interpretation

First of all, it is important to realise that the effect of pores (rounded surfaces) and cracks (sharp crack tips) on mechanical strength are different. Sharp crack tips reduce the mechanical strength much more than pores. Thus, the formation of channel cracks is expected to decrease the mechanical strength much more than the presence of pores.

Furthermore, it is important to bear in mind that the appearance of the fracture surfaces reflects two cracking events, (i) crack faces forming during cool down

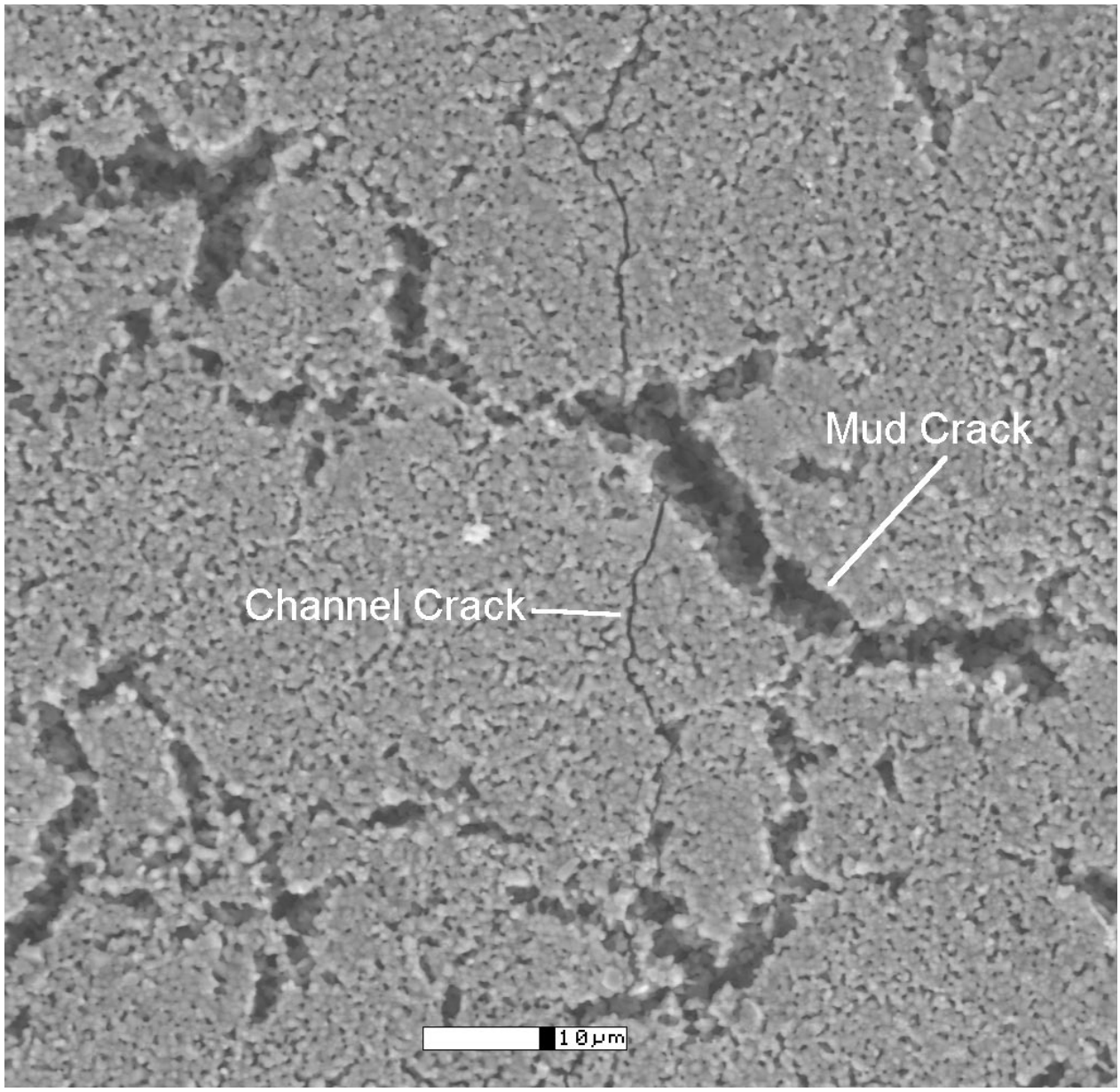

(a)

Figure 2 ESEM micrographs of a specimen sintered at 1300 °C, showing (a) the surface of the coating, and (b) the fracture surface. Note the presence of cracks in the coating (a). Note also, that there is no interfacial debonding; the fracture surface of the substrate follows that of the coating.

(hereafter denoted 'pre-existing cracks') and (ii) cracking as the specimen was broken by external load. Obviously, it is impossible to determine exactly which part of the fracture surface that originate from pre-existing cracks and which part that has formed during breakage of the specimen. However, the distinctively different appearance of the fracture surfaces allows us to obtain the key information on the relationship between the fracture mode and strength.

The cause for the formation of channel cracks is assumed to be residual stresses originating from the difference in the thermal expansion coefficients of the two materials. Assuming that the layers sinter together stress free at the processing temperature, residual stresses build up in the multilayers during cooling, as the layers are bonded to each other, and cannot contract freely.

The residual stresses that build up in the coating layers are *tensile*, since the thermal expansion coefficient of the coating, α_c, exceeds that of the substrate, α_s (see Table I [6, 9–10]). If the residual tensile stresses are sufficiently high, channel cracks can form in the coating.

TABLE I Thermo-elastic properties of the materials [6, 9, 10]

	Material	E (GPa)	ν	$\alpha(\times 10^{-6}/^{\circ}\mathrm{C})$
Substrate	YSZ	200	0.3	10.8
Coating	NiO/YSZ	∼50	∼0.3	12.3

Another issue is the bonding across the interface between coating and substrate. If the fracture energy of the interface is sufficiently low, a channel crack in the coating will deflect along the interface, resulting in delamination. If crack deflection does not occur, the crack can propagate into the substrate.

Returning now to the experiments, we note the following: For specimens sintered at 1100 °C, the substrate

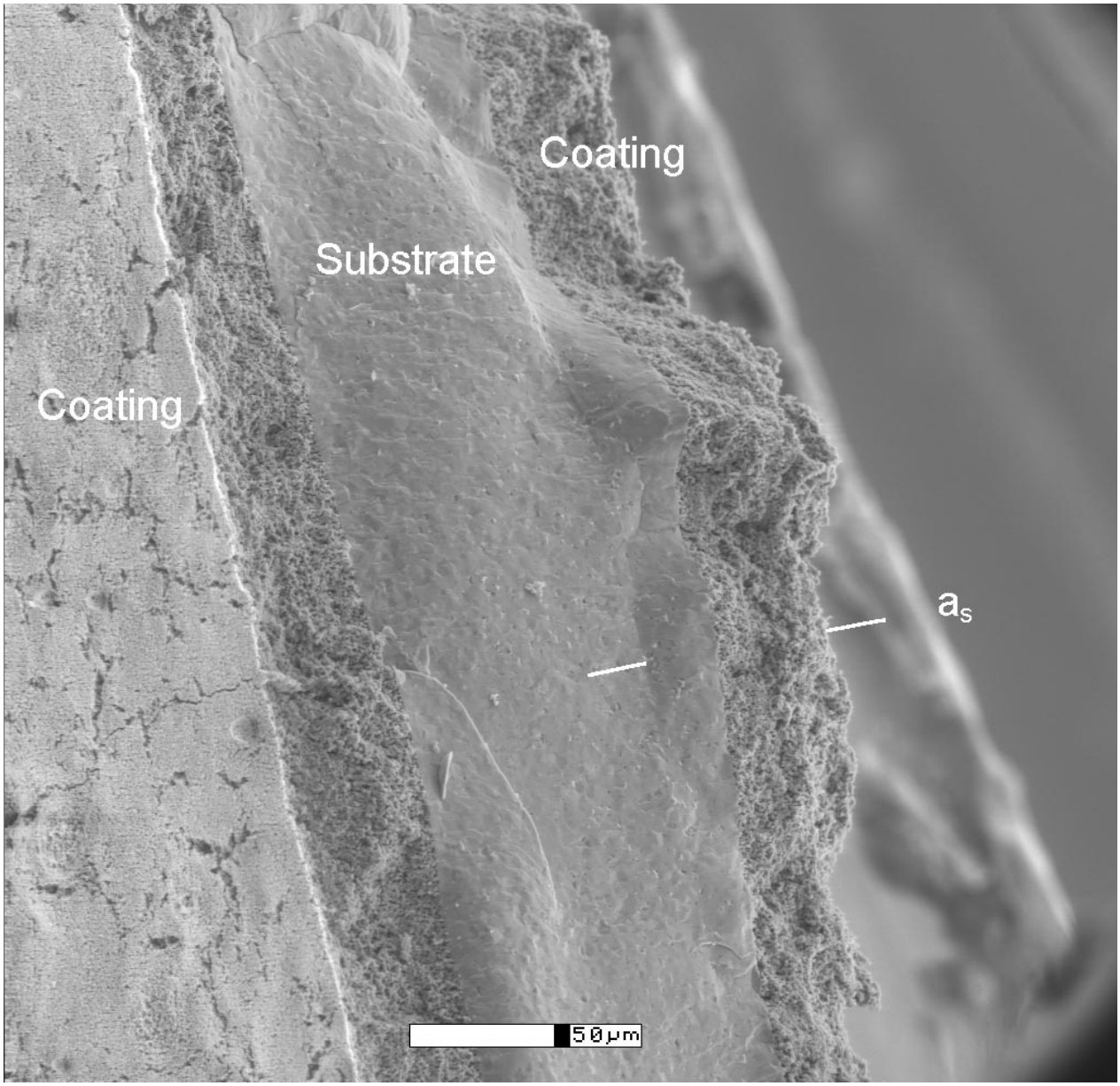

(b)

Figure 2 (Continued)

fractures along a plane, different from the coating. Thus, fractures of the two materials are two independent events. Cracks in the coating cannot enter the substrate, instead delamination occurs. Fracture of the substrate requires the initiation of a crack from a flaw in the substrate, exactly as for blank YSZ. This is likely to be the reason why the fracture strength of coated YSZ sintered at 1100 °C is similar to that of blank YSZ.

In contrast, no interface debonding is observed for specimens sintered at 1300 °C and 1500 °C, indicating that for these specimens the interface bonding is so strong that crack deflection cannot occur. Thus, cracks that have formed in the coating layers can propagate into the substrate. Then truly sharp cracks (pre-existing cracks) are present *in the substrate* after cool down. The fracture strength of specimens with pre-existing cracks is likely to be much lower than that of pure YSZ, which contains small flaws, but no sharp cracks. The assumed cracking and fracture modes are shown in Fig. 5. Since the residual stresses are highest for the specimens sintered at the highest temperature, it is likely that the channel cracks penetrate deeper into the substrate for the specimens sintered at 1500 °C. Consequently, these specimens have the lowest strength.

4. Comparison with fracture mechanics models

4.1. Basic assumptions and limitations

Apparently, all fracture mechanics models for channel cracking concerns a thin coating on a substrate having a thickness that is much larger than that of the coating. In the present experiments the substrate thickness, H, is larger than the thickness of the coating, h, but they are of the same order of magnitude. Furthermore, in the present experiments coatings were deposited on both faces of the substrate. Nevertheless, the models based on infinite thick substrates are assumed to be qualitative

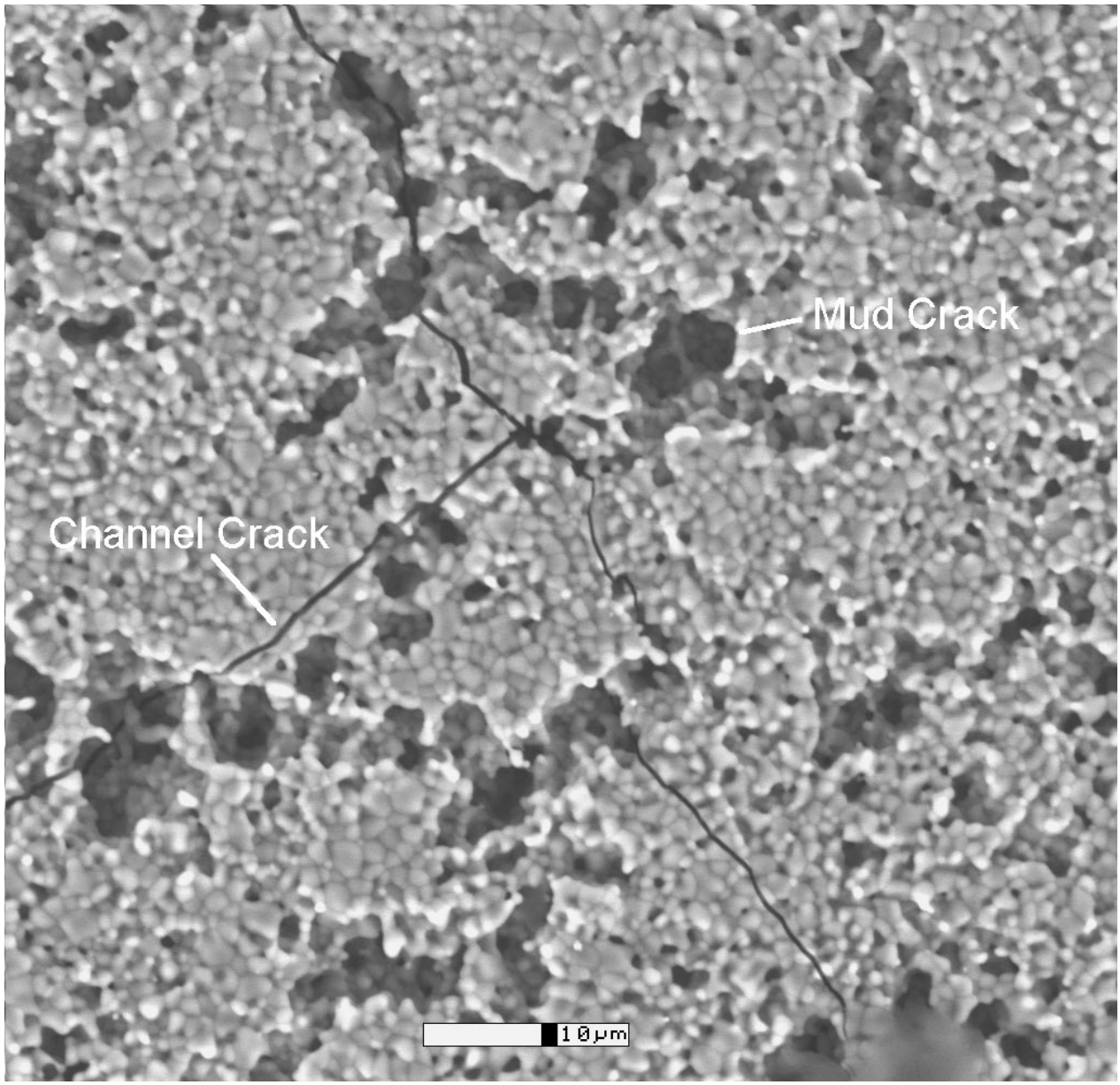

(a)

Figure 3 ESEM micrographs of a specimen sintered at 1500 °C, showing (a) the surface of the coating, and (b) the fracture surface. Cracks are present in the coating. The fracture surface is irregular.

correct for the present problem, and in the following we will use such models to corroborate the interpretation presented above.

4.2. Channel cracks

Analysis reveals that channel cracking of a coating layer on a thick substrate is a steady-state problem; the energy release rate attains a steady-state value once the crack length becomes just a few times the coating thickness [11]. Thus, extensive cracking can occur when the steady-state energy release rate of the channel crack, $\mathcal{G}_{\mathrm{ch}}$, equals (or exceeds) the critical energy release rate (the fracture energy) of the coating, $\mathcal{G}_{\mathrm{c,c}}$. $\mathcal{G}_{\mathrm{ch}}$ is related to the residual stress in the coating, σ_{c}, and the thickness of the coating, h, as [8]

$$\mathcal{G}_{\mathrm{ch}} = \Omega(D_\alpha, D_\beta)\frac{\sigma_{\mathrm{c}}^2 h}{E_{\mathrm{c}}}, \tag{1}$$

where $\bar{E}_{\mathrm{c}} = E_{\mathrm{c}}(1-\nu_{\mathrm{c}}^2)$ is the plain strain modulus, E_{c} is the Young's modulus and ν_{c} is the Poisson's ratio of the coating. Ω is a non-dimensional function that only depends on the elastic properties of coating and substrate; Ω can be described by two nondimensional stiffness parameters D_α and D_β (the Dundurs' parameters). For plane strain conditions they are [12]

$$D_\alpha = \frac{\bar{E}_{\mathrm{c}} - \bar{E}_{\mathrm{s}}}{\bar{E}_{\mathrm{c}} + \bar{E}_{\mathrm{s}}} \quad D_\beta = \frac{\mu_{\mathrm{c}}(1-2\nu_{\mathrm{s}}) - \mu_{\mathrm{s}}(1-2\nu_{\mathrm{c}})}{2\mu_{\mathrm{c}}(1-\nu_{\mathrm{s}}) + 2\mu_{\mathrm{s}}(1-\nu_{\mathrm{c}})}, \tag{2}$$

where μ denotes the shear modulus, $\mu = E/2(1+\nu)$. The subscripts indicate material (c is coating and s is the substrate). The function $\Omega(D_\alpha, D_\beta)$ can be obtained from the analysis of Beuth [8]. Using the material data giving in Table I the Dundurs' parameters become $D_\alpha = -0.6$ and $D_\beta = -0.17$. Then Ω becomes 1.36.

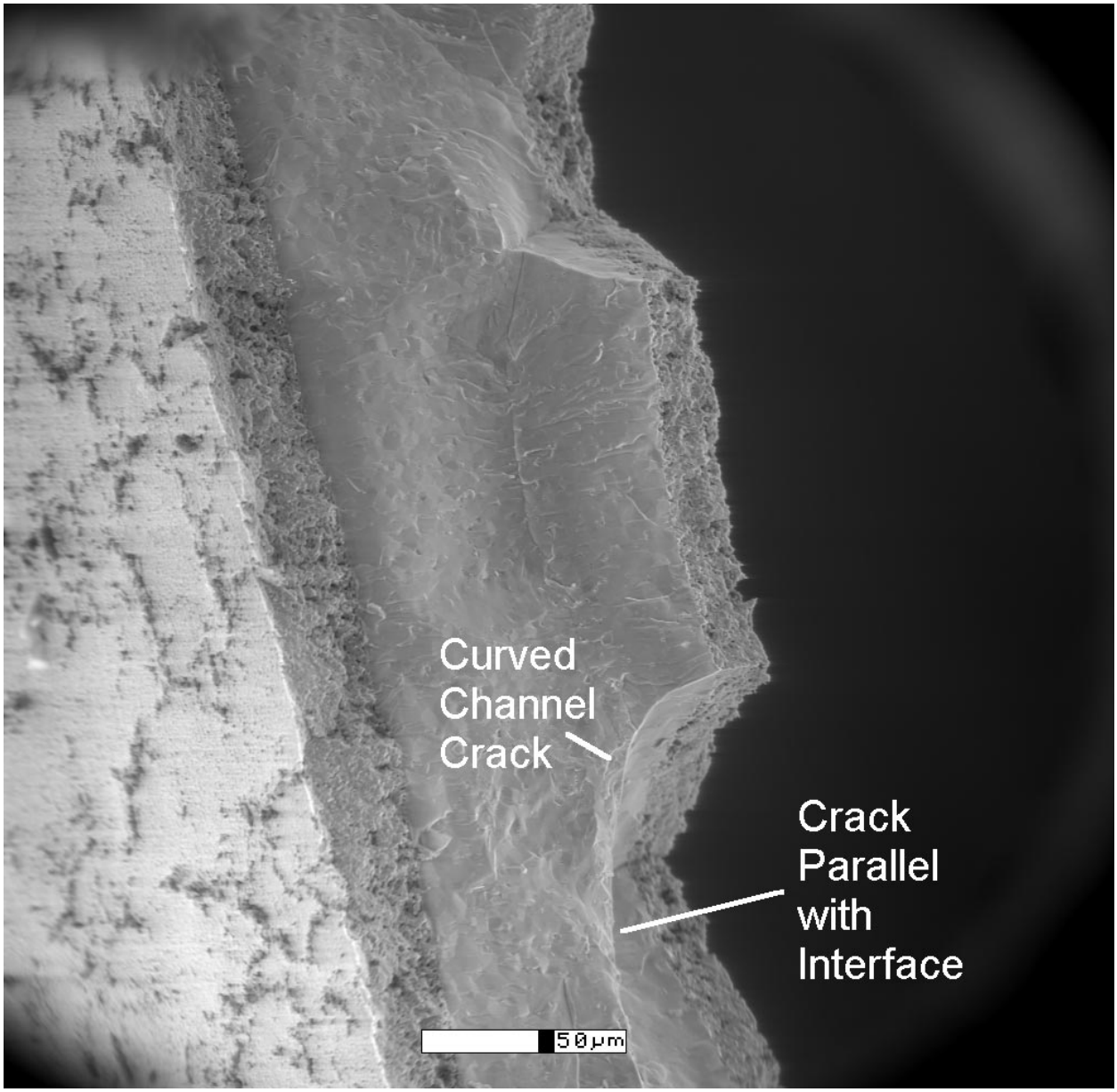

(b)

Figure 3 (Continued)

Assuming again an infinite thick substrate, the residual stress in the coating, σ_c, at temperature T is

$$\sigma_c = (\alpha_c - \alpha_s)(T_p - T)E_c/(1 - \nu_c), \qquad (3)$$

where T_p is the processing (sintering) temperature at which the multilayer is assumed to be stress free. For the present materials $\alpha_c > \alpha_s$ (Table I) and $T_p > T$, so that σ_c is positive (tensile). The calculated values of $\mathcal{G}_{ch}$ are listed in Table II. Since thermally induced cracks were found for $T_p = 1300\,^{\circ}\mathrm{C}$ (but not for $T_p = 1100\,^{\circ}\mathrm{C}$) we can estimate $\mathcal{G}_{c,c} \approx 12\ \mathrm{J/m^2}$.

TABLE II Fracture mechanical results

T_p (°C)	$\mathcal{G}_{ch}$ (J/m^2)	a_s/h (calculated)	a_s/h (measured)
1100	10	2.5	0
1300	14	3.5	1–2
1500	19	4.0	3–4

4.3. Crack deflection or propagation?

Once channel cracks have formed in the coating, the next question is whether they will propagate into the substrate or deflect along the interface. This question can be answered by use of the model by He and Hutchinson [13]. Crack deflection will occur if the fracture energy of the interface, $\mathcal{G}_{i,c}$, is sufficiently small in comparison with the fracture energy of the substrate, $\mathcal{G}_{s,c}$. Neglecting the residual stresses in the substrate, the criterion for crack deflection is, when $D_\alpha = -0.6$ [13],

$$\mathcal{G}_{i,c}/\mathcal{G}_{s,c} < 0.5. \qquad (4)$$

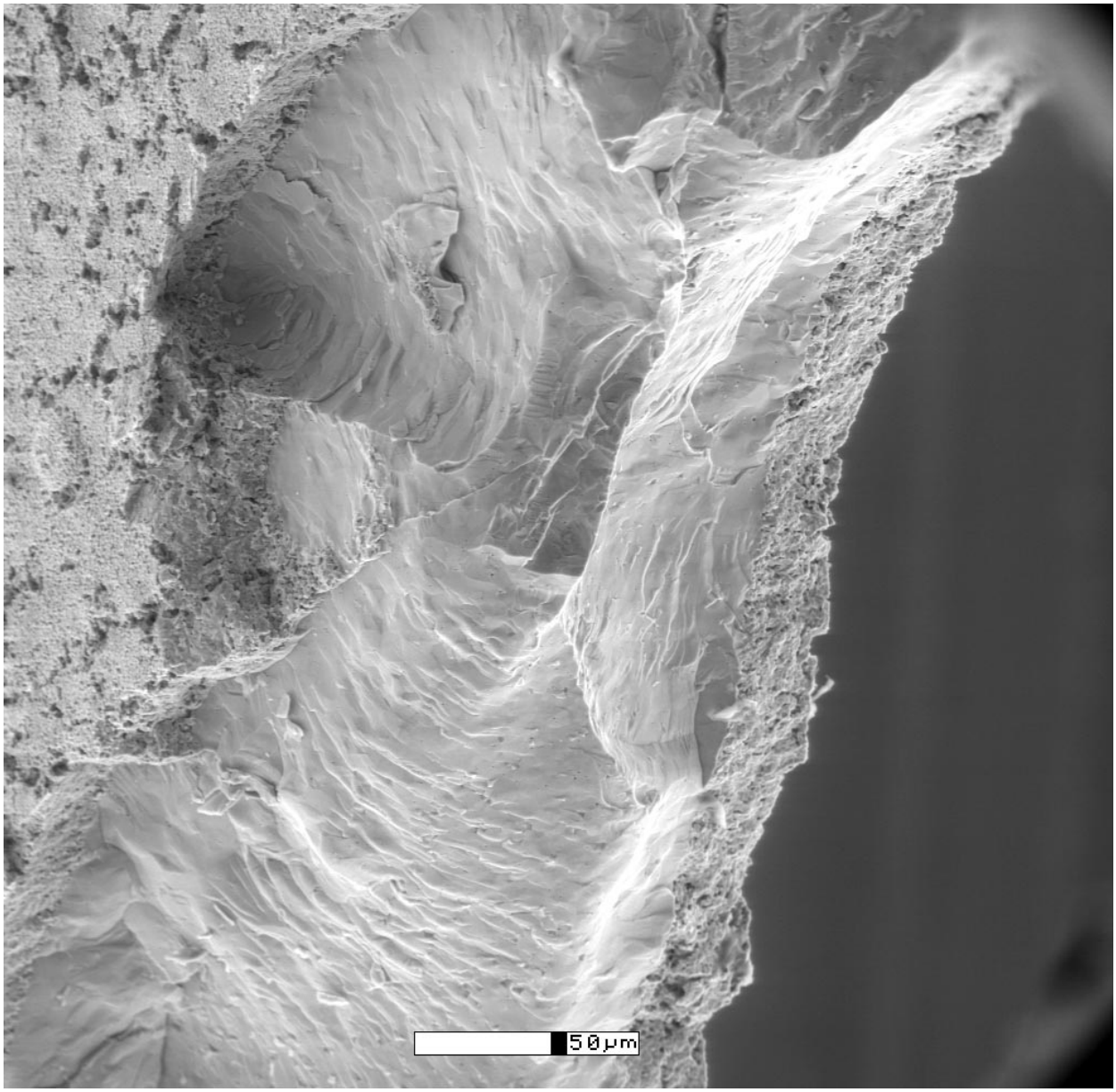

Figure 4 ESEM micrographs of the fracture surface of a specimen sintered at 1500 °C. Note how cracks have grown into the substrate and changed direction to grow parallel with the interface.

A lower limit for the fracture energy of YSZ is $\mathcal{G}_{s,c} \approx 3$ J/m^2 [6]. Thus, crack deflection should occur if $\mathcal{G}_{i,c} < 1.5$ J/m^2. The experiments suggest that the crack deflection criterion (4) is fulfilled for the specimen sintered at 1100 °C, but not for the specimens sintered at 1300 and 1500 °C. It is plausible that the higher sintering temperature results in an enhanced bonding between the coating and substrate, i.e., a higher $\mathcal{G}_{i,c}$.

4.4. Crack penetration into the substrate

The next issue is how deep cracks penetrate into the substrate. This problem has been studied by Ye *et al*. [14] for the case of infinite thick substrates. We assume that in our experiments the crack penetration depth is equal to the depth of the boundary zone seen in Fig. 3b. The measured crack penetration depth, a_s, is shown in Table II along with predictions from the model of Ye *et al*. [14]. The trends of the experimental results are in agreement with the predictions of the model. The differences in the experimental and model values are attributed to the fact that the models are based on an infinite thick substrate; for the multilayers examined the thickness of the substrates is just a few times that of the coating.

The final question is why channel cracks, once they have grown into the substrate, change direction and propagate in the substrate parallel with the interface. To answer this question, we recall that a crack in a homogenous material usually chooses a path where no shear stresses exist just ahead of the crack tip, the so-called pure mode I path [15]. Channel cracks, extend perpendicular to the interface, are mode I cracks. But whether or not a crack path in a homogenous material is directional stable depends on the normal stress component acting parallel with the crack plane, the so-called T-stress [16]. If the T-stress is < 0 (compression), the crack growth is directional stable, whereas if the

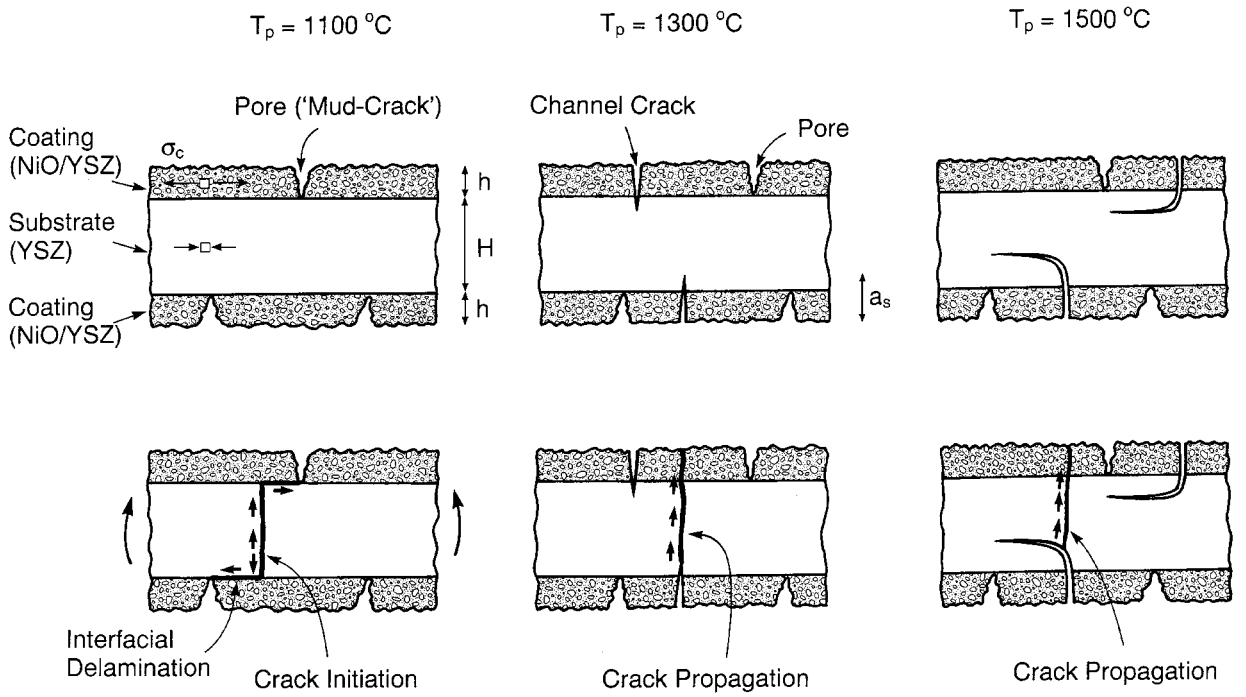

Figure 5 A schematic showing the assumed cracking modes due to residual stresses (top) and the resulting fracture mode for specimens subjected to bending (below). Sintering temperatures are given above the figure.

T-stress is > 0 (tension) the crack growth direction is unstable, and the crack may bend or kink. Ye *et al.* [14] analysed the problem of a channel crack propagating from the coating into the substrate. They showed that the T-stress is positive when the Dundurs parameter $D_\alpha < 0$ (which is the case here).

Thus, for the present materials a channel crack from the coating propagating into the substrate is directionally unstable. Crack kinking is thus likely to occur. The crack will then grow parallel with the interface at a certain distance from the interface, at the location where a pure mode I path exists [17]. For a thin coating on a thick substrate the mode I path lies a distance of about $h/2$ below the film when $D_\alpha = -0.6$ [17]. However, for the present problem (coatings on both faces on a substrate with a thickness in the same order of magnitude as the coatings) it may be anticipated that a mode I path exists in the symmetry plane of the specimen.

5. Discussion

5.1. Related problems

The present problem is in line with a property transition found for continuous fibre reinforced ceramics. At low temperatures such composite are damage tolerant; multiple matrix crack can form without causing composite fracture. During multiple matrix cracking the fibres remain intact, because crack deflection occurs at the fibre/matrix interfaces. At intermediate and high temperatures these fibre composites can loose their damage tolerant behaviour due to the formation of a strong interfacial bonding between fibres and matrix [18].

The present problem has also similarities with the behaviour of ceramics with weak layers subjected to external loadings. Clegg and co-workers [19, 20] studied the mechanical behaviour of multilayers with weak layers being subjected to bending. It was found that 'weak' interfaces between the ceramic layers could cause crack deflection. Failure of the next layer requires the initiation of a new crack in the layer. Thus, the presence of weak interfaces can change the failure mode significantly.

5.2. Comparison of fracture energies

Finally, a comment is given on the estimated value of fracture energy of the coating ($\mathcal{G}_{c,c} \approx 12$ J/m^2). The fracture energy of the porous coating is somewhat higher than the fracture energy of the substrate ($\mathcal{G}_{s,c} = 3$ J/m^2 [6]). It may be surprising that a porous material can have higher fracture energy than a dense material. However, the relative magnitude of $\mathcal{G}_{c,c}$ and $\mathcal{G}_{s,c}$ can be cross checked, utilising the fact that specimens sintered at 1300 °C exhibited channel cracks that had propagated into the substrate. If $\mathcal{G}_{c,c}$ had been (much) smaller than $\mathcal{G}_{s,c}$, the channel cracks would have stopped at the interface. The channel cracks did propagate into the substrate, suggesting that $\mathcal{G}_{c,c} > \mathcal{G}_{s,c}$.

6. Conclusions

Experimental work has shown that multilayer components consisting of a YSZ substrate coated with a NiO/YSZ composite have a high mechanical strength when the multilayers are sintered at 1100 °C, and a low strength when they are sintered at 1300 °C or 1500 °C. Fracture mechanics models suggest that the loss of strength is due to two phenomena: (i) The development of cracks in the coating due to stresses originating from thermal expansion mismatch and (ii) an increase in the interfacial fracture energy with increasing sintering temperature. Then cracks in the coating can penetrate

into the YSZ substrate and act as truly sharp cracks. The presence of these sharp crack tips in the substrate results in a much lower strength.

Acknowledgements

The authors acknowledge financial support from the Danish SOFC research programme (DK-SOFC) under Danish Ministry of Energy. BFS was partly supported by the Risø Engineering Science Centre for Structural Characterisation and Modelling of Materials. Discussions with Dr. Carsten Bagger and Dr. Andy Horsewell are acknowledged.

References

1. S. P. S. BADWAL and K. FOGER, *Materials Forum* **21** (1997) 187.
2. J. D. FRENCH, H. M. CHAN, M. P. HARMER and G. A. MILLER, *J. Amer. Ceram. Soc.* **79** (1996) 58.
3. D. STOLTEN, H. STARK and W. SCHÄFER, First Int. Symp. on New Metals for Fuel Cell Systems, Montreal, Canada (1995) p. 1.
4. M. BROCCO, G. COSOLI, L. PILLONI and M. RONCHETTI, in Proc. 1st European Solid Oxide Fuel Cells Forum, edited by U. Bossel, Lucerne, Switzerland, (1994) p. 767.
5. H. L. TOFTEGAARD, A. N. KUMAR and B. F. SØRENSEN, unpublished research (1997).
6. A. N. KUMAR and B. F. SØRENSEN, *J. Amer. Ceram. Soc.* (1998) submitted.
7. C. BAGGER, In *1992 Fuel Cell Seminar* Program and Abstracts, Nov. 29–Dec. 2, 1992, Tucson, AZ, Courtesy Associates, Inc., Washington DC, USA, (1992) p. 241.
8. J. L. BEUTH, *Int. J. Solids Structures* **29** (1992) 1657.
9. P. V. HENDRIKSEN, private communication, 1997.
10. M. MORI, T. YAMAMOTO, H. ITOH, H. INABA and H. TAGAWA, *J. Electrochem. Soc.* **145** (1998) 1374.
11. T. NAKAMURA and S. KAMATH, *Mechanics of Materials* **13** (1992) 67.
12. J. DUNDURS, *J. Appl. Mech.* **36** (1969) 650.
13. M.-Y. HE and J. W. HUTCHINSON, *Int. J. Solids Structures* **25** (1989) 1053.
14. T. YE, Z. SUO and A. G. EVANS, *ibid.* **29** (1992) 2639.
15. M. D. THOULESS and A. G. EVANS, *Scripta Metall. Mater.* **24** (1990) 1507.
16. B. COTTERELL and J. R. RICE, *Int. J. Fracture* **16** (1980) 155.
17. Z. SUO and J. W. HUTCHINSON, *Int. J. Solids Structures* 25 (1989) 1337.
18. K. M. PREWO, *J. Mater. Sci.* **21** (1986) 3590.
19. J. W. CLEGG, *Acta Metall. Mater.* **40** (1992) 3085.
20. A. J. PHILLIPS, W. J. CLEGG and T. W. CLYNE, *ibid.* **41** (1992) 805.

Received 31 August
and accepted 18 September 1998